

**Dieses Dokument ist eine Zweitveröffentlichung (Verlagsversion) /
This is a self-archiving document (published version):**

Matthias Roth, Jörg Heber, Klaus Janschek

**Concept for the fast modulation of light in amplitude and phase using
analog tilt-mirror arrays**

Erstveröffentlichung in / First published in:

SPIE OPTO. San Francisco, 2017. Bellingham: SPIE, Vol. 10116 *[Zugriff am: 23.05.2019]*.

DOI: <https://doi.org/10.1117/12.2250746>

Diese Version ist verfügbar / This version is available on:

<https://nbn-resolving.org/urn:nbn:de:bsz:14-qucosa2-351249>

„Dieser Beitrag ist mit Zustimmung des Rechteinhabers aufgrund einer (DFGgeförderten) Allianz- bzw. Nationallizenz frei zugänglich.“

This publication is openly accessible with the permission of the copyright owner. The permission is granted within a nationwide license, supported by the German Research Foundation (abbr. in German DFG).

www.nationallizenzen.de/

PROCEEDINGS OF SPIE

[SPIDigitalLibrary.org/conference-proceedings-of-spie](https://spiedigitallibrary.org/conference-proceedings-of-spie)

Concept for the fast modulation of light in amplitude and phase using analog tilt-mirror arrays

Matthias Roth, Jörg Heber, Klaus Janschek

Matthias Roth, Jörg Heber, Klaus Janschek, "Concept for the fast modulation of light in amplitude and phase using analog tilt-mirror arrays," Proc. SPIE 10116, MOEMS and Miniaturized Systems XVI, 101160H (20 February 2017); doi: 10.1117/12.2250746

SPIE.

Event: SPIE OPTO, 2017, San Francisco, California, United States

Concept for the fast modulation of light in amplitude and phase using analog tilt-mirror arrays

Matthias Roth^a, Jörg Heber^b, and Klaus Janschek^a

^aTechnische Universität Dresden, Institute of Automation, 01062 Dresden, Germany

^bFraunhofer Institute for Photonic Microsystems, Maria-Reiche-Str. 2, 01109 Dresden, Germany

ABSTRACT

The full complex, spatial modulation of light at high frame rates is essential for a variety of applications. In particular, emerging techniques applied to scattering media, such as Digital Optical Phase Conjugation and Wavefront Shaping, request challenging performance parameters. They refer to imaging tasks inside biological media, whose characteristics concerning the transmission and reflection of scattered light may change over time within milliseconds. Thus, these methods call for frame rates in the kilohertz range. Existing solutions typically offer frame rate capabilities below 100 Hz, since they rely on liquid crystal spatial light modulators (SLMs). We propose a diffractive MEMS optical system for this application range. It relies on an analog, tilt-type micro mirror array (MMA) based on an established SLM technology, where the standard application is grayscale amplitude control. The new MMA system design allows the phase manipulation at high-speed as well.

The article studies properties of the appropriate optical setup by simulating the propagation of the light. Relevant test patterns and sensitivity parameters of the system will be analyzed. Our results illustrate the main opportunities of the concept with particular focus on the tilt mirror technology. They indicate a promising path to realize the complex light modulation at frame rates above 1 kHz and resolutions well beyond 10,000 complex pixels.

Keywords: Diffractive Optics, Spatial Light Modulators, Phase Modulation, Micro-optical Devices

1. INTRODUCTION

Spatial beam shaping plays an important role in a variety of optical applications. Recently, new techniques dealing with strongly scattering media, such as wavefront shaping¹ and digital optical phase conjugation^{2,3} focus light inside and through opaque media and promise to create new imaging and photo manipulation instruments. In order to reach that goal, they call for spatial light modulators (SLMs) with framerates in the kHz range, the full complex field modulation of intensity and phase, a pixel resolution above 10,000 and reasonable photon efficiencies. According to the current state, a general solution for that purpose appears still to be identified.⁴

Bearing in mind the high-speed requirement, some of the interesting candidates are SLMs based on micro-electro-mechanical systems (MEMS) that support kilohertz or even megahertz framerates. As a prominent example, a recent study has considered the digital micromirror device (DMD)⁵ as an option for complex-valued beam shaping. Extended Lee-holography, or a “superpixel” method,⁶ may transform the DMD response directly into a phase and intensity profile. Therefore, complex beam shaping at frame rates up to 30 kHz seems possible. Limitations associated with the binary amplitude principle nevertheless lead to the boundary that about 8 x 8 tilt mirrors are necessary to form one complex-valued image point. Consequently, Lee-holography based methods reduce the resolution of the DMD. This effect is also reflected by the optical efficiency that has been reported below 1 % or up to 4 % in Ref. 6.

Numerous phase forming experiments rely on liquid crystal, membrane or piston-type MEMS mirror arrays. Our proposition of using tilt mirror arrays may seem like an unusual technology choice, because prior studies apply these devices exclusively for the generation of intensity images. This situation becomes more clear recognizing

Further author information: (Send correspondence to M.R.)

E-mail: matthias.roth@tu-dresden.de, Telephone: +49 351 46332243

that the number of fast piston modulators available for scientific experiments, namely MEMS piston mirror arrays with more than 10,000 pixel and framerates > 1 kHz, seems to be virtually zero, still. Conversely, tilt mirror arrays reach pixel numbers of more than one million and feature frame rates up to the MHz range.⁷ New projects with MEMS piston mirror arrays as outcome are to be expected in the next years based on the research momentum of the wavefront shaping community worldwide.⁴ In the meantime, new ideas are certainly welcome to further approach and support the initial experimental goals.

The present article studies an optical system concept for complex beam shaping based on tilt-mirror arrays. They are in focus based on their inherent high-speed capability as well as their public availability. The study concentrates on “analog” tilt mirror arrays, i.e. each single mirror may continuously change its torsion state. Our main interest is the question, how the analog degree of freedom may be exploited to modulate a complex image field with fewest possible tilting mirrors. We analyze the modulation properties of an appropriate optical system based on diffraction simulation and illustrate the new opportunities as well as limits of the cell-based imaging arrangement.

We would like to emphasize that T. Sandstrom has already published an original technique, how analog MEMS mirror arrays, including tilt-mirrors, can be designed to control amplitude and phase.⁸ This path clearly addresses the design and manufacturing of new MEMS mirror arrays. In our case, we intend to limit on existing tilt-mirror arrays that are available for experiment. The present study therefore considers aspects of the optical system with a specific static phase element to prepare the optical MMA response for wavefront shaping or holography. The additional static element can be realized e.g. as a diffractive optical element.

2. TILT-MIRROR-BASED MODULATION IN AMPLITUDE AND PHASE

2.1 Diffractive tilt-mirror arrays

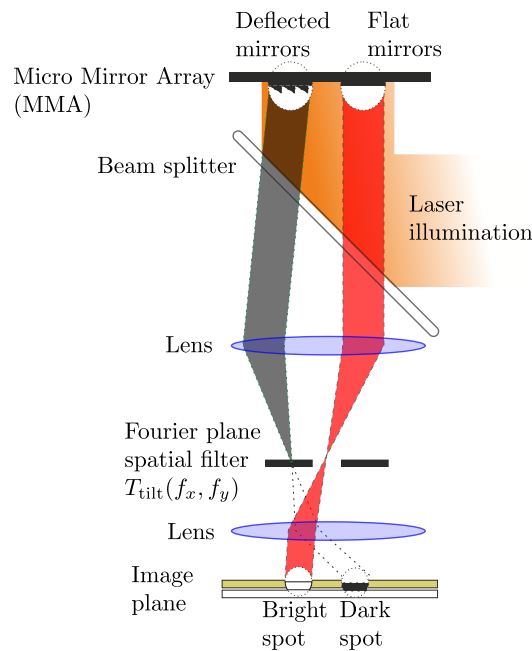


Figure 1: Optical setup for amplitude modulation based on tilt-mirror arrays.

A typical application of analog micromirror arrays (MMAs) is their utilization as programmable grayscale mask,⁹ as illustrated in Figure 1. The diffractive mirror array creates a pure phase profile, which an optical 4f-setup converts to an intensity image by means of Fourier filtering. As sketched in Figure 1, mirrors in the flat state generate a bright spot in the image plane. Deflected mirrors fulfilling the so-called blaze condition may create dark spots. They diffract all incident light to the first diffraction order that gets absorbed by an

aperture in the Fourier plane. Mirrors at intermediate tilt angles partially diffract the light to the absorbing Fourier aperture and thereby enable intermediate intensity levels or “grayscale spots” in the image plane. The simulation of the optical MMA response typically considers a reflective device, where the MMA surface profile $h(y)$ and the wave number k determine the optical phase $\phi(y)$ (see Figure 2a):

$$\phi(y) = 2kh(y) \tag{1}$$

Within the Fraunhofer approximation, the field response of each mirror u_{tilt} at the image plane can be derived from the tilt angle θ according to eq.(2), where we assume appropriate filtering. We define the dimensionless factor ζ to normalize the behavior of the device with respect to different wavelengths λ and pixel pitches p and may write:

$$u_{\text{tilt}}(\theta) \propto \frac{\sin(\zeta\pi)}{\zeta\pi} \text{ with } \zeta = \frac{2p \tan(\theta)}{\lambda} \tag{2}$$

The mirrors may diffract light generally into the first and also higher diffraction orders. A spatial amplitude filter in the Fourier plane may block these components. Using spatial frequency coordinates in the Fourier plane,¹⁰ we express the aperture transmission filter T_{tilt} as:

$$T_{\text{tilt}}(f_y) = \text{rect}\left(\frac{f_y}{2f_{b,y}}\right) \text{ with } f_{b,y} < \frac{1}{p}, \tag{3}$$

where the maximum bandwidth $f_{b,y}$ for absorbing the first diffraction order is given by the inverse of the pixel pitch p . Figure 2b illustrates the mirror’s field response in the image plane u_{tilt} as a function of the tilt angle. Equivalently, Figure 2c sketches the projection of this response in the complex plane. The field modulation is purely real. The plot shows that tilt mirrors can generate negative amplitude values (180 degree phase shift) with about 20 % of the maximum positive amplitude.

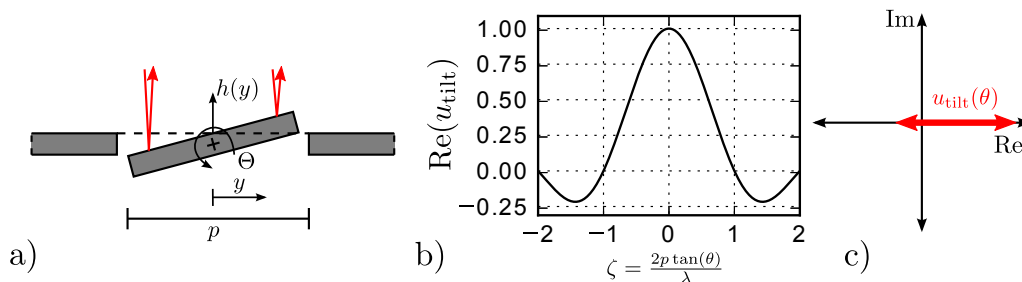


Figure 2: Illustrations of a) a tilt mirror pixel and b) field response as a function of the tilt parameter ζ . c) modulation path in the complex plane.

2.2 System concept for the full complex modulation of light

We consider a multi-pixel technique to generate an arbitrary complex field in the image plane. A 4f-setup with an adapted Fourier filter may realize the overlay of grouped MMA pixels to an array of “macro”-pixels in the image plane. Particularly, we incorporate a static phase element (SPE) in the system close to the MMA or in a conjugated optical plane. This allows creating virtually any desired field response using the grouped tilt-mirrors. We refer to such a group of pixels from now as a complex modulation cell (CMC). Figure 3 shows an overview, how the 4f Fourier filter converts the phase modulation of the CMC into an arbitrary phase-intensity modulation. The SPE in front of the MMA contributes to the complex modulation by rotating the pixels’ field responses in the complex plane (see Figure 3b). After the optical overlay, any complex response vector will be accessible in the image field. Let us have a look at a CMC consisting of 4 x 1 analog tilt mirrors. One particular SPE configuration is a phase-shift of each individual CMC pixel by $\pi/2$ compared to the neighbor. Accordingly, four

different phase shifts apply to the image amplitude. The output field follows from the sum of the phase-shifted pixel fields $u_{p,i}$:

$$u_{\text{cmc}} = \sum_i u_{p,i} = u_{\text{tilt},1} \exp(j0) + u_{\text{tilt},2} \exp(j\pi/2) + u_{\text{tilt},3} \exp(j\pi) + u_{\text{tilt},4} \exp(j3\pi/2) \quad (4)$$

Figure 3 sketches this example and the specific SPE phase shifts in detail. Please note that the light passes the SPE twice in Figure 3a, so that it effectively implements the phase shifts of eq.(4). Figure 3b and c indicate how the superposition of the 4 phase-shifted MMA pixels may create the image response in the whole complex range. The three steps of

1. Defining an initial phase profile by a CMC of tilt mirrors
2. Adding the specific SPE phase shift and
3. Superposing the phase modulation with an optical system (Fourier filter)

form a flexible concept to generate arbitrary complex field vectors with analog tilt-mirror's CMC (Figure 3c).

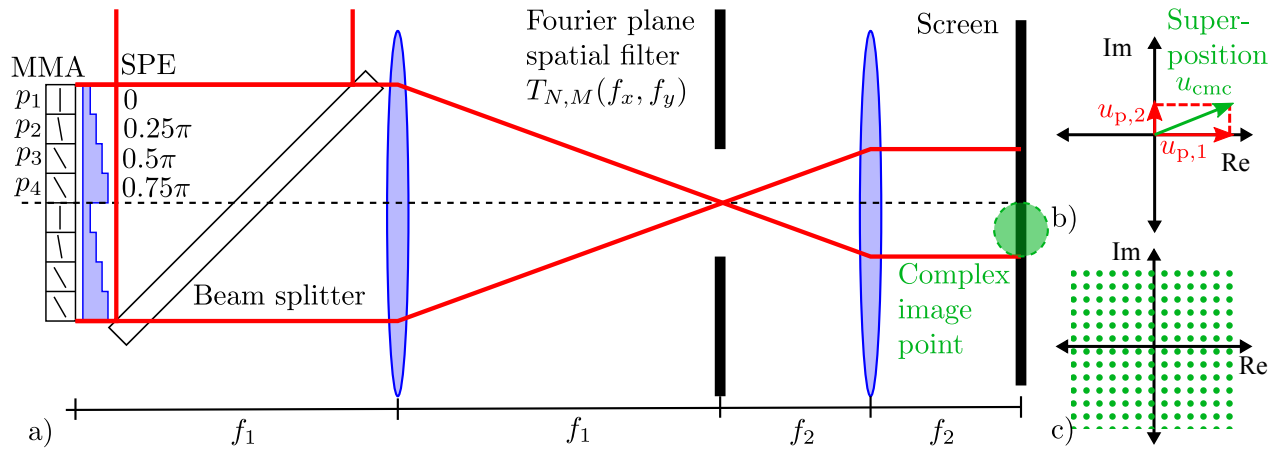


Figure 3: a) Schematic optical setup consisting of a tilt mirror SLM, a static phase element (SPE), a beam splitter (BS), and two lenses with aperture to realize a spatial low-pass filter. The figure shows a complex modulation cell CMC of 4 x 1 pixels arranged in a line. b) Interference vector of phase-shifted pixel contribution. c) Range of complex modulation assuming 7 tilt levels for all single mirrors.

The simulation of such a system can be straightforwardly carried out. Within the limits of Fraunhofer diffraction,¹⁰ we may write the field distribution in the Fourier plane based on a Fourier transform:

$$u_{\text{diff}}(f_x, f_y) = \mathfrak{F}(\exp(j(\phi_{\text{slm}}(x, y) + \phi_{\text{spe}}(x, y)))) \quad (5)$$

where ϕ_{slm} is the phase modulation of the MMA and ϕ_{spe} is the static phase operator. Considering the spatial filter T and the second lens' Fourier transform, the output field u_{out} reads:

$$u_{\text{out}}(x, y) = \mathfrak{F}(u_{\text{diff}}(f_x, f_y)T(f_x, f_y)) \quad (6)$$

The shape of the T aperture in the Fourier plane has to exclude all diffraction orders outside the main optical path. Assuming the main axis as the zero order, one can define the aperture transmission for a CMC consisting of $N \times M$ pixels with pitch p as:

$$T_{N,M} = \text{rect}\left(\frac{f_x}{2f_{b,x}}, \frac{f_y}{2f_{b,y}}\right) \text{ with } f_{b,x} < \frac{1}{Np}, f_{b,y} < \frac{1}{Mp} \quad (7)$$

Effectively, this is a low-pass filter, which increases the size of a diffraction-limited spot to at least the size of the CMC.

3. TILT-MIRROR MODULATION - TWO EXAMPLES

The proposed setup leaves the freedom to choose any desired CMC shape and size. In the first section, we consider a square CMC with a minimum pixel number. Section 3.2 includes additional “sub-pixel” phase structures in the simulation.

3.1 Complex beam shaping with analog tilt MMAs and a symmetric CMC

Let us consider a square CMC consisting of 2×2 micromirrors. Figure 4a illustrates the characteristic phase profiles of the MMA and SPE. The expected image amplitude is $u_{\text{cmc}} = 1/4 \exp(j\pi)$. The CMC’s shape suggests a square Fourier filter and thereby guarantees symmetric resolutions in both image directions. As a suitable choice of the filter size we assume half the bandwidth of eq.(7). This filter choice considers simulations where a perfect (spatial) coherent illumination is supposed. As a consequence, the image spot will be 2×2 CMCs during the present simulations.

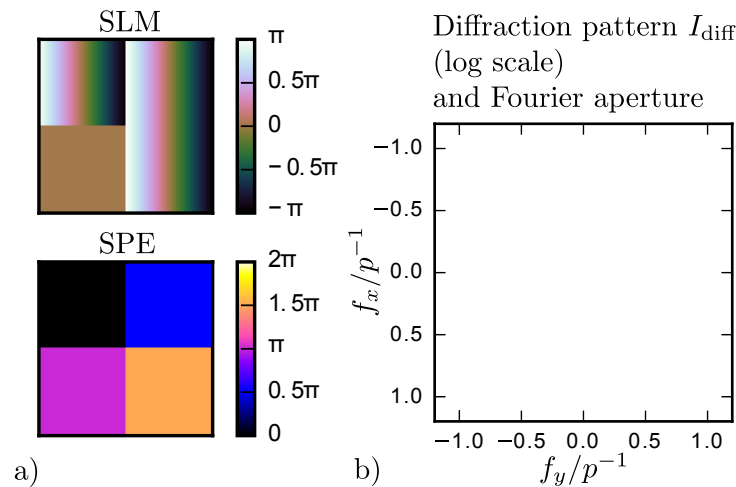


Figure 4: Simulated modulation in amplitude and phase based on a 256×256 tilt-mirror array. a) CMC consisting of 2×2 MMA tilt-mirrors and SPE with 4 phase levels. b) Diffraction pattern showing distinct diffraction orders.

Of course, experiments may also utilize almost the full bandwidth of eq. (7) at a later stage and thereby increase the resolution. In that case optimized partially coherent or incoherent illumination conditions come into view which are beyond the objective of the present simulation.

The diffraction pattern in Figure 4b shows the Fourier plane intensity with distinct diffraction orders. Only the zero order propagates to the output.

Figure 5 illustrates the result of a complete diffraction simulation based on such a MMA/SPE configuration. The MMA model is a publicly available 256×256 tilt-mirror device.¹¹ Two distinct test patterns¹² define the target image and monitor the amplitude and phase channels. We have converted the target images to a resolution of 128×128 pixels in order to account for the virtual, complex-valued system resolution in the image plane (2×2 pixels). Bearing in mind the mentioned Fourier filter shape, the size of the diffraction-limited image spot increases to 4×4 pixels and the final image actually comprises 64×64 complex-valued image points.

Comparing the expected field maps with the simulated system output, promising image fidelity for both amplitude and phase can be seen. Clearly, the tilt-mirror array can indeed modulate amplitude and phase within the system. The phase channel is remarkably clear while certain diffraction artifacts appear in the amplitude image. Typically, the high-frequency components in the phase profile may cause these artifacts. One can expect these for every diffractive technique. They are a direct consequence of the restriction of the space-bandwidth by the spatial filter.

In summary, this first MMA/SPE test-configuration indicates that very small cells of 2×2 tilt-mirrors may

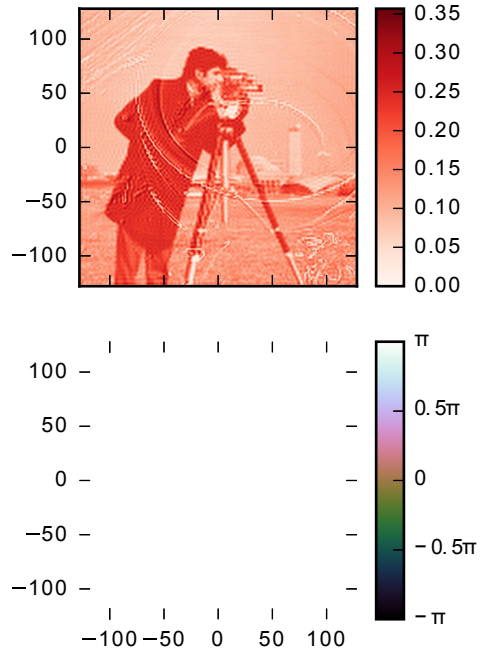


Figure 5: Simulated optical output of complex modulation based on a 256x256 tilt-mirror array.

support the complex modulation tasks. The analog MMA control can be exploited to significantly increase the image resolution.

3.2 Beam shaping with quasi phase-step mirrors and asymmetric CMC

A special class of diffractive MEMS is the so-called phase-step mirror.¹³ Its main feature is the capability to increase the negative amplitude range of conventional tilt MMAs. Phase-step mirrors can be manufactured by incorporating a height step of $\lambda/4$ along the tilt axis of each mirror.

With the present study, we propose to consider phase-step mirrors in the context of a MMA/SPE system design as new conception. On the one hand, its availability becomes strongly simplified with the SPE concept. A standard tilt MMA can be applied without changes. Additionally, only a specialized SPE with a subpixel-structure, namely a mask step along the tilt axis (see Figure 6a), is necessary and strongly reduces the effort of potential MEMS processing steps. We are interested in how the complex beam shaping may take advantage of the “quasi” phase-step response, i.e. by incorporating “subpixel” structures in the SPE. We express the phase-step term $\phi_{ps}(y)$, which we incorporate in the SPE, as:

$$\phi_{ps}(y) = \pi \operatorname{rect} \left(\frac{y \bmod p - 0.75p}{0.5p} \right) \quad (8)$$

This MMA/SPE-modification changes the field response of a pixel to the analytical function $u_{ps}(\theta)$:

$$u_{ps}(\theta) = j \frac{\cos(\zeta\pi) - 1}{\zeta\pi} \quad \text{with } \zeta = \frac{2p \tan(\theta)}{\lambda} \quad (9)$$

Possible values of $u_{ps}(\theta)$ consist of positive and negative amplitudes with a maximum of roughly $\pm\sqrt{0.5}$ each (see Figure 6b). With that background, we may define a suitable CMC for complex beam shaping. Only two tilt mirrors will suffice to modulate the entire complex plain, since one “quasi” phase-step mirror already covers one axis in the complex plane. Compared to the former section, the phase step modification significantly increases

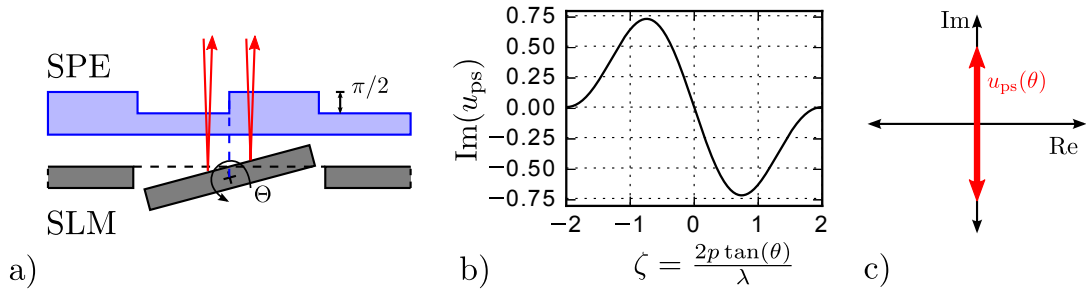


Figure 6: Illustration of "quasi" phase-step mirrors: a) Schematic, b) Modulation curve as a function of the tilt parameter ζ . c) Modulation curve in the complex plane.

the number of CMCs for a given MMA-device and thus increases the effective resolution. The 1 x 2 CMC will be asymmetric this time, which affects the output resolution as well. We assume the low-pass filter as slit aperture accordingly:

$$T_{1,2}(f_y) = \text{rect}\left(\frac{f_y}{2f_{b,y}}\right) \text{ with } f_{b,y} < \frac{1}{2p}. \quad (10)$$

Again, half of the maximum filter size might be a suitable choice for initial simulations with coherent illumination. Figure 7a shows the phase profile of an asymmetric 1 x 2 CMC, where the SPE implements $\pi/2$ subpixel phase steps in addition to a $\pi/4$ phase difference between the two neighboring pixels. In the Fourier plane, the diffraction orders are blocked in one direction, based on the slit aperture.

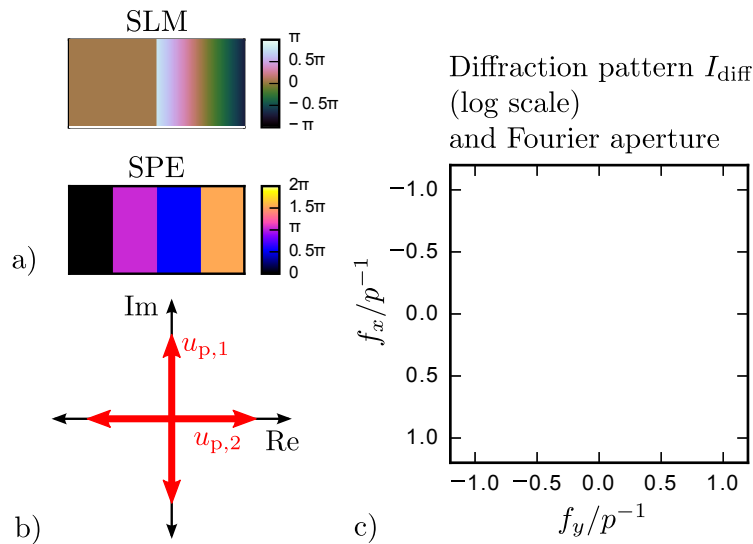


Figure 7: a) Asymmetric CMC based on 1 x 2 MMA tilt-mirrors and subpixel SPE phase step modification. b) Modulation range of the 2 quasi phase-step mirrors. c) Diffraction pattern showing distinct diffraction orders and slit filter.

Figure 8 illustrates the results of our optical simulation using, again, the 256 x 256 MMA. SLM and SPE now form 256 x 128 CMCs. The Fourier filter creates a diffraction-limited image spot of 1 x 4 pixels. The effective resolution increases to 256 x 64 complex-valued image points. Comparing the simulation result with expected field maps of Figure 5, again promising image fidelity for both amplitude and phase can be seen. The phase image seems accurate, as in the previous example. Few diffraction artifacts appear in the amplitude

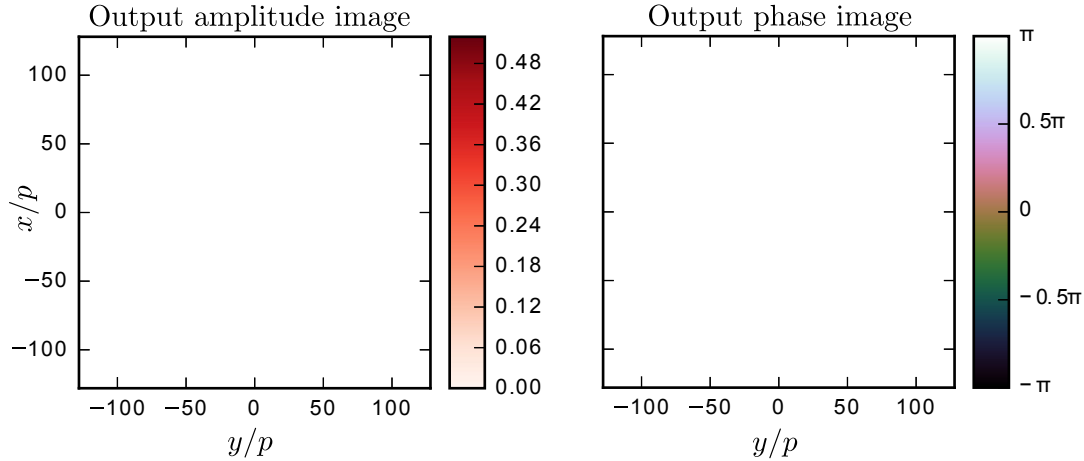


Figure 8: Diffraction simulation based on a 256 x 256 tilt-mirror array and a SPE that realizes “phase steps”.

image. However, now it shows reduced artifacts, particularly in the x-direction where the slit filter does not restrict the light propagation. This illustrates the increase of effective resolution in the case of quasi phase-step mirrors.

In summary, the second test-configuration proves that only two tilt-mirrors of a MEMS-array may realize the complex modulation task. The MMA/SPE concept seems to be effective. This time, not only the analog MMA control has been exploited to increase the image resolution. Particularly, also the subpixel-profile seems to be a promising design option that may strongly enhance the complex field modulation.

4. APPLICATION PROPERTIES

4.1 Optical efficiency

The utilization of analog MMAs may increase the spatial resolution. The former sections have shown progress in the range of one order of magnitude compared to previous techniques. Simultaneously, the optical throughput of the modulation system is of utmost importance. The efficiency of the MMA/SPE concept can be defined within the complex modulation space. Considering Figure 3b, the largest circle inside the addressable space determines the optical efficiency. Every single pixel may reach this radius at its maximum amplitude A_{\max} of the tilt trajectory. The intensity efficiency η of an arbitrary CMC with size $N \times M$ therefore reads:

$$\eta = \left(\frac{A_{\max}}{NM} \right)^2 \quad (11)$$

The previous examples draw the following picture:

- The case of a symmetric 2 x 2 CMC (section 3.1) defines the complex radius of modulation by a mirror amplitude of $1/4 = 0.25$ (4 mirrors per cell), which corresponds to an intensity efficiency of 6.25 %. Additionally, negative amplitude contributions might be incorporated in the modulation. The maximum amplitude increases in that case (20 % negative amplitude) and enhances the efficiency to 9 %.
- The second case of an asymmetric 1 x 2 CMC with quasi phase-step mirrors indicates another scenario. The modulation amplitude by a single mirror reaches about $\pm 0.5\sqrt{0.5}$ and doubles the efficiency to ≈ 12.5 %.
- As final example and variation of the former points, a symmetric 2 x 2 CMC of quasi phase-step mirrors seems interesting. By defining the SPE with an appropriate interpixel-shift of $\pi/8$ (instead of $\pi/4$ for the 1 x 2 CMC), this configuration reaches an intensity efficiency of ≈ 18 %. The already promising efficiency of the “1 x 2” CMC obviously can be enhanced with potential for further improvement.

This overview illustrates that small CMCs may strongly improve the system performance not only in spatial resolution. The intensity efficiency remains at least comparable to the DMD case or even surpasses that state. At the moment, a variety of CMCs are to be analyzed and an upper limit of efficiency cannot be stated. Nevertheless, the efficiency range approaches 20 %, which is well above binary tilt-mirror solutions and further improvement can be expected.

4.2 Adjustment sensitivity

The current modulation concept relies on the precise alignment of the static phase element (SPE) and the SLM. In order to estimate the positioning tolerance, we have simulated the generation of a plane wave with MMA/SPE local variation. We analyze the mean of the output intensity as a function of the lateral SPE translation Δx relative to the SLM pitch p . The numerical simulation uses 200×200 data points per tilt mirror as reasonable sampling resolution. Without loss of generality, the array size has been reduced to 20×20 pixels, based on the elementary target wave.

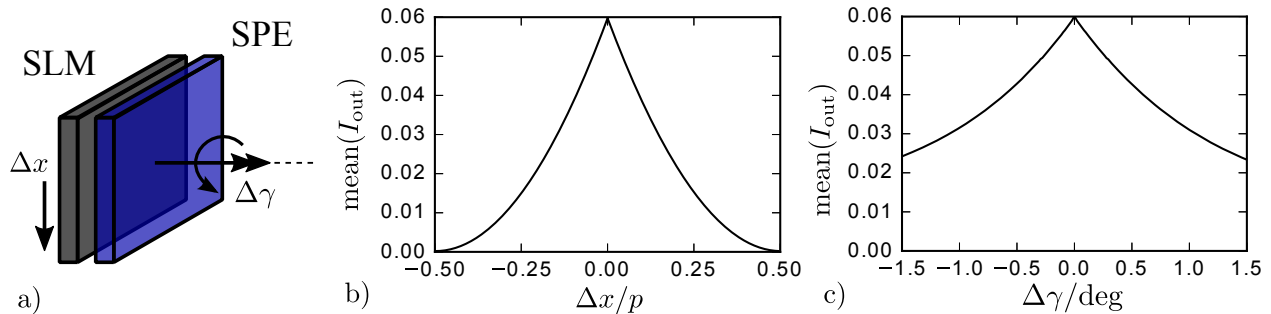


Figure 9: Sensitivity of lateral and rotational misalignments. a) Illustration of simulation geometry. b) Mean intensity of a plane wave as a function of lateral SPE-displacement. c) Influence of rotational misalignment.

Figure 9b shows the variation of the modulation output as a function of the mechanical alignment. A positioning accuracy below $p/20$ will be necessary if 20 % or less intensity variation will be expected. Similarly, the in-plane rotation $\Delta \gamma$ affects the modulation quality, as displayed in Figure 9c. The former intensity tolerance of I_{out} requires an axial alignment below ± 0.3 deg, which reflects the pixel tolerance in the angular direction for the small mirror array.

As a result, tight requirements for a proper MMA/SPE alignment are visible. The precise arrangement of both MMA and SPE nevertheless seems feasible. Two possibilities exist for the SPE arrangement in the optical setup a) in a conjugated image plane or alternatively b) “close” to the MMA. Option (a) enables a quick start for laboratory experiments where positioning elements with submicron tolerance are available. Furthermore, option (b) opens the door to manufacture the MMA/SPE combination directly as one single device within existing MEMS processes. The corresponding overlay of MEMS processing typically may reach submicron accuracy and therefore meets the MMA/SPE requirements.

4.3 Spectral application

The present system design uses the MMA/SPE combination to concentrate the complex beam modulation in the zero diffraction order. In difference to that, previous work deals with higher diffraction orders that create a setup with an angularly shifted optical axis.⁶ Technically, the zero order facilitates the alignment of the optical setup on a well-defined axis and is a practical argument for the convenient system alignment.

Furthermore, the utilization of the zero order suggests itself as a key feature for spectral application. The whole optical path remains the same by changing the illumination wavelength. The MMA is programmable and directly supports a sequence of illumination wavelengths, i.e. multispectral operation appears feasibly. In that case, the SPE can be mechanically exchanged or even replaced by a programmable version like a second SLM. Assuming the spectral variation to be sufficiently slow, a LCD or LCOS SLM with appropriate resolution might serve that purpose.

5. SUMMARY

The present study on tilt-mirror arrays holds good news for complex beam shaping. For the first time, cells of tilt-mirrors as small as 2×2 pixels (or less) have been demonstrated to enable amplitude as well as phase control. The key feature is the concept of combining fast SLMs with a static phase mask (SPE). It enables to take advantage of the analog modulation of diffractive (tilt) micromirror arrays as the essential degree of freedom to increase the spatial resolution. Furthermore, our results suggest that subpixel features may strongly improve both the effective resolution and the modulation efficiency. A test arrangement indicates an efficiency of 18 % for a symmetric quasi-phase-step mirror cell. This is, to the best of our knowledge, the highest efficiency reported until now for tilt-mirrors. An increase of that preliminary result can be expected in future work. Last but not least, the proposed utilization of the zero diffraction order opens a door even for spectral application.

Besides its prospects, the modulation concept sets clear requirements for the system alignment. The effort of the MMA/SPE overlay appears achievable with state-of-the-art equipment, i.e. the price of an additional SPE alignment might be affordable compared to the gain of application advantages.

In conclusion, diffractive tilt-mirror arrays appear as promising candidates for the complex beam shaping with high spatial resolution and speed. Future work is interested in their upper limit of efficiency and experimental testing based on MMAs available as an evaluation kit.¹¹

REFERENCES

- [1] Vellekoop, I., “Feedback-based wavefront shaping,” *Optics Express* **23**(9) (2015).
- [2] Yaqoob, Z., Psaltis, D., Feld, M., and Yang, C., “Optical phase conjugation for turbidity suppression in biological samples,” *Nat. Photon.* **2**(2) (2008).
- [3] Horstmeyer, R., Ruan, H., and Yang, C., “Guidestar-assisted wavefront-shaping methods for focusing light into biological tissue,” *Nature Photonics* **9**, 563–571 (Aug. 2015).
- [4] Gigan, S., “Optical microscopy aims deep,” *Nat Photon* **11**, 14–16 (Jan. 2017).
- [5] Dudley, D., Duncan, W. M., and Slaughter, J., “Emerging digital micromirror device (DMD) applications,” in [*Proc. SPIE*], **4985**, 14–25, International Society for Optics and Photonics (2003).
- [6] Goorden, S., Bertolotti, J., and Mosk, A., “Superpixel-based spatial amplitude and phase modulation using a digital micromirror device,” *Opt. Express* **22**(15) (2014).
- [7] Schmidt, J.-U., Dauderstaedt, U. A., Duerr, P., Friedrichs, M., Hughes, T., Ludwig, T., Rudloff, D., Schwaten, T., Trenkler, D., Wagner, M., Wullinger, I., Bergstrom, A., Bjoernangen, P., Jonsson, F., Karlin, T., Ronnholm, P., and Sandstrom, T., “High-speed one-dimensional spatial light modulator for Laser Direct Imaging and other patterning applications,” in [*Proc. SPIE*], **8977**, 89770O (Mar. 2014).
- [8] Sandström, T., “Spatial light modulator with structured mirror surfaces, international publication number wo 2009/130603 a2,” (2009).
- [9] Heber, J., Kunze, D., Dürr, P., Rudloff, D., Wagner, M., Björnängen, P., Luberek, J., Berzinsh, U., Sandström, T., and Karlin, T., “Contrast properties of spatial light modulators for microlithography,” in [*Proceedings of SPIE*], Naber, R. J. and Kawahira, H., eds., **6730**, 673035–673035–10 (Oct. 2007).
- [10] Goodman, J. W., [*Introduction to Fourier optics*], Roberts, Englewood, Colo., 3 ed. (2005).
- [11] Berndt, D., Heber, J., Sinning, S., Kunze, D., Knobbe, J., Schmidt, J.-U., Bring, M., Rudloff, D., Friedrichs, M., Rössler, J., Eckert, M., Kluge, W., Neumann, H., Wagner, M., and Lakner, H., “Multispectral characterization of diffractive micromirror arrays,” in [*Proc. SPIE*], **7718**, 77180Q–77180Q–11 (2010).
- [12] van der Walt, S., Schönberger, J. L., Nunez-Iglesias, J., Boulogne, F., Warner, J. D., Yager, N., Gouillart, E., Yu, T., and the scikit-image contributors, “scikit-image: image processing in Python,” *PeerJ* **2**, e453 (6 2014).
- [13] Sandstrom, T. and Ljungblad, U. B., “Phase-shifting optical maskless lithography enabling ASICs at the 65- and 45-nm nodes,” in [*Proc. SPIE*], **5567**, 529 (Dec. 2004).